

Asteroseismology of the β Cephei stars

II. 12 (DD) Lacertae

W.A. Dziembowski^{1,2} and M. Jerzykiewicz³

¹ Warsaw University Observatory, al. Ujazdowskie 4, PL-00-478 Warsaw, Poland

² Copernicus Astronomical Center, Polish Academy of Sciences, ul. Bartycka 18, PL-00-716 Warsaw, Poland (e-mail: wd@astrouw.edu.pl)

³ Wrocław University Observatory, ul. Kopernika 11, PL-51-622 Wrocław, Poland (e-mail: mjerz@astro.uni.wroc.pl)

Received 11 August 1998 / Accepted 21 October 1998

Abstract. Five pulsation modes are simultaneously excited in this well-known β Cephei star. Three of them, including the one with the largest light and radial-velocity amplitudes, form a triplet. The triplet is equidistant in frequency to within the errors of measurement, that is, 0.0003 d^{-1} .

Explaining why the triplet should be so nearly equidistant turns out to be a real challenge to the theory. We investigate the following three options: (1) rotational splitting, (2) an oblique magnetic pulsator, and (3) nonlinear phase lock. Unfortunately, apart from the frequencies, the data are meager. Photometric indices yield the effective temperature and surface gravity of rather low accuracy. In addition, the existing determinations of the spherical harmonic degree of even the strongest observed mode are discrepant. Consequently, the model parameters are not well constrained.

We show that of the three above-mentioned options, the oblique pulsator model is unlikely because it would require excessively strong dipolar field or a special field geometry. The rotational splitting is a possibility, but only for an $\ell = 2, p_0$ mode in a model with specific values of the effective temperature and surface gravity. Finally, we note that the nonlinear phase lock may be the solution. However, verifying this depends on the progress of nonlinear calculations.

Key words: stars: individual: DD Lac – stars: interiors – stars: oscillations – stars: variables: general

1. Introduction

The first paper of this series (Dziembowski & Jerzykiewicz 1996, henceforth Paper I) was devoted to the β Cephei star 16 (EN) Lacertae. Presently we turn to 12 (DD) Lac = HR 8640, one of the longest known variables of this type. The star was discovered to have variable radial-velocity by Adams (1912). The main period of the variation, equal to $0^{\text{d}}.193089$, was derived by Young (1915). This value was confirmed by all subsequent investigators. Young (1915) has also noticed that the amplitude

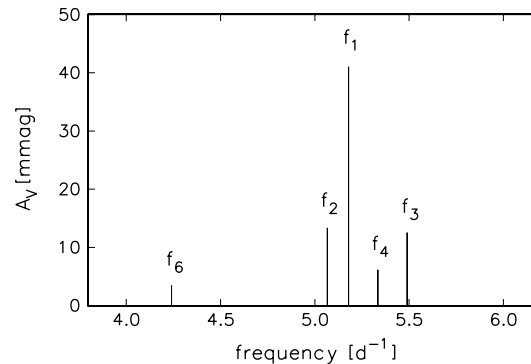


Fig. 1. Frequency spectrum of 12 (DD) Lac: the amplitudes of five harmonic terms are plotted as a function of frequency. The combination term, $f_5 = f_1 + f_4$, is not shown

and the phase of maximum of the velocity curve vary from cycle to cycle.

The variability of brightness of 12 (DD) Lac was discovered photoelectrically by Stebbins (1917) and Guthnick (1919). The photometric period turned out to be equal to Young's spectrographic one. The light-curve also showed the cycle-to-cycle variations.

Following this early work, 12 (DD) Lac was the subject of numerous investigations, including the classic work of Struve (1951) and an international observing campaign organized in 1956 by de Jager (Abrami et al. 1957, de Jager 1963). A review of observations of 12 (DD) Lac throughout 1977 has been given by Jerzykiewicz (1978). The most recent references are Mathias et al. (1994), Pigulski (1994), and Aerts (1996).

All modern analyses agree that the above-mentioned cycle-to-cycle variations of the star's radial-velocity and light curves result from interference of six harmonic terms. The frequencies of five of them are confined to a narrow interval from about 4.2 to 5.5 d^{-1} . The amplitudes of these five terms, derived by Jerzykiewicz (1978) from the 1956 V -magnitude observations of Abrami et al. (1957), are plotted in Fig. 1 as a function of frequency. The terms are numbered in the order of decreasing amplitude. The frequency of the fifth term, not shown in the

figure, is equal to the sum of the first and the fourth, $f_5 = f_1 + f_4$. The frequencies f_1 , f_4 , and f_3 form an equidistant triplet.

In Sect. 2 we present the data: the star's position in the $\log T_{\text{eff}} - \log g$ plane, the frequencies, and the available determinations of the spherical harmonic degrees, ℓ , and orders, m , of the observed modes. Details of deriving $\log g$ can be found in the Appendix. In Sect. 3 we consider three possibilities of accounting for the equidistant triplet. As in Paper I, we limit the analysis to $\ell \leq 2$. Sect. 4 contains the summary.

2. Data

2.1. The effective temperature

The MK spectral type of 12 (DD) Lac is B 1.5 III (Lesh 1968). Five stars of similar MK type (that is, spectral type B 1 or B 2 and luminosity class from IV to II) are among the 32 stars for which Code et al. (1976) determined the empirical effective temperatures from the OAO-2 absolute fluxes and the intensity interferometer angular diameters. A mean $\log T_{\text{eff}}$ for these five stars is equal to 4.369, and a mean of the standard deviations is 0.017.

Another value of $\log T_{\text{eff}}$ can be obtained from the Strömngren c_0 and β indices. Using the recent calibration of Napiwotzki et al. (1993) and the observed c_0 and β of 12 (DD) Lac (Sterken and Jerzykiewicz 1993, Table 2A), we get $\log T_{\text{eff}} = 4.380$.

The mean of the above two values, equal to 4.374, we shall adopt as $\log T_{\text{eff}}$ of 12 (DD) Lac. Note, however, that since Napiwotzki et al. (1993) based their calibration on the empirical effective temperatures of Code et al. (1976), the two values are independent of each other only insofar as different observations of 12 (DD) Lac were used to derive them. Taking into account the mean standard deviation of the empirical $\log T_{\text{eff}}$ values and uncertainties of the MK type and photometric indices, we estimate the standard deviation of the $\log T_{\text{eff}}$ value we adopted to be equal to 0.020.

2.2. Surface gravity

Using solar-composition model atmospheres of Kurucz (1979) and procedures of Schmidt & Taylor (1979) and Schmidt (1979), Smalley & Dworetzky (1995) computed a grid of synthetic Strömngren β indices as a function of T_{eff} and $\log g$. In the Appendix we check this grid against empirical $\log g$ values of early-B components of several binary systems and then derive $\log g$ of 12 (DD) Lac from its observed β index. The value we obtained is 3.76 ± 0.15 .

In Fig. 2, 12 (DD) Lac is plotted using the above-mentioned values of $\log T_{\text{eff}}$ and $\log g$ as coordinates. Also shown in the figure are evolutionary tracks computed by means of the new version of the Warsaw-New Jersey stellar evolution code with the updated OPAL opacities (Iglesias & Rogers 1996) for $X = 0.7$ and $Z = 0.02$. The code assumes uniform rotation and global angular momentum conservation and takes into account averaged effects of the centrifugal force. For the tracks shown in Fig. 2, and for all models that will be discussed below, the

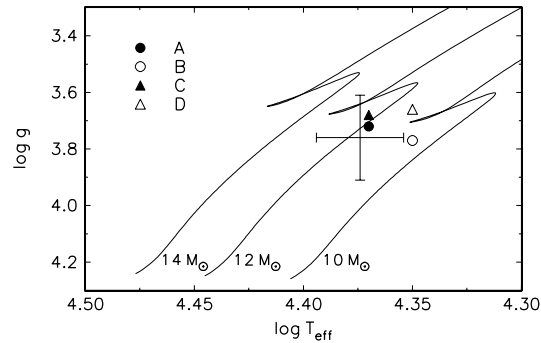


Fig. 2. 12 (DD) Lac (crossed error bars) in the $\log T_{\text{eff}} - \log g$ plane. The solid lines are evolutionary tracks computed by means of the Warsaw-New Jersey stellar evolution code with updated OPAL opacities (Iglesias & Rogers 1996) for $X = 0.7$ and $Z = 0.02$. The models A, B, C and D are discussed in Sect. 3.1

Table 1. Observed pulsation frequencies of 12 (DD) Lac

i	f_i [d $^{-1}$]	Δf_i [d $^{-1}$]
1	5.17897	0.00008
2	5.06634	0.00006
3	5.48985	0.00040
4	5.33427	0.00005
6	4.24091	0.00010

equatorial velocity of rotation on the ZAMS, $V_{\text{rot},0}$, is assumed to be equal to 100 km s^{-1} .

2.3. The frequencies

The observed values of the frequencies we shall use for comparison with computed eigenfrequencies are given in the second column of Table 1. They are equal to $1/P_i$, where P_i are the mean periods derived by Pigulski (1994) from all available photometric and radial-velocity data. We omitted the combination frequency, $f_5 = f_1 + f_4$.

Pigulski (1994) has also investigated the secular stability of the amplitudes and periods of the six terms. The only variation he detected in the amplitudes was a 30 percent increase of the light amplitude of the second term between 1961 and 1983. On the other hand, he found all six periods to vary on time scales comparable with the total span of the data, that is, about 75 years. The variations have very small amplitudes, however. The relative amplitudes, estimated from Pigulski's (1994) Fig. 1 and expressed in terms of frequency, are given in the third column of Table 1. They can be regarded as observational uncertainties of the frequencies.

2.4. The discrepant ℓ values

For the f_1 term, the spherical harmonic degree, ℓ , has been recently derived from the observed light, colour and radial-velocity amplitudes by Cugier et al. (1994). Using nonadiabatic eigenfunctions of Dziembowski & Pamyatnykh (1993), Cugier

et al. (1994) examined diagnostic properties of several diagrams with different amplitude ratios as coordinates. They showed that modes of different $\ell \leq 2$ are particularly well resolved when the colour to light amplitude ratio, A_{U-V}/A_V , is used as abscissa, and the radial-velocity to light amplitude ratio, K/A_V , as ordinate. In this diagram, the f_1 term falls on the $\ell = 1$ sequence.

For the f_2 term, the 1962–1976 *UBV* photometry of Sato (1973, 1977, 1979) and all available radial-velocities (Pigulski 1994) yield $A_{U-V}/A_V = 0.41 \pm 0.14$ and $K/A_V = 489 \pm 42$ $\text{km s}^{-1} \text{mag}^{-1}$. In the above-mentioned diagnostic diagram of Cugier et al. (1994), these coordinates indicate $\ell = 1$ or 2, but certainly not $\ell = 0$.

From the same data, the amplitude ratios for the f_3 term are $A_{U-V}/A_V = 0.80 \pm 0.17$ and $K/A_V = 353 \pm 34$ $\text{km s}^{-1} \text{mag}^{-1}$. Unfortunately, a point with these coordinates lies outside the $\ell \leq 2$ area in the diagnostic diagram: while the first ratio falls within the range of abscissa corresponding to $\ell = 0$, the second one is more than five standard deviations below the smallest $\ell = 0$ ordinate. However, if the first ratio were decreased by two standard deviations, the point would move into the $\ell = 1$ sequence. Since a decrease by four standard deviations would be required to reach the $\ell = 2$ sequence, we conclude that $\ell = 1$ is the best identification for f_3 from the amplitude ratios now available.

For the remaining terms, f_4 and f_6 , the errors of the amplitude ratios become so large that discrimination between different ℓ values is no longer possible.

The above identifications can be compared with the results obtained from the line-profile observations. Unfortunately, the three modern line-profile studies of 12 (DD) Lac yield conflicting results although they were all based on observations of the Si III $\lambda\lambda$ 4553–4575 lines. Smith (1980) maintains that his data can be accounted for only if the triplet terms are identified with the $\ell = 2$, $m = 0, -1, -2$ states and the f_2 mode is assumed to be radial, while Mathias et al. (1994) conclude that the f_1 mode is either a sectoral one or a tesseral one with $\ell - 1 = |m|$. More recently, the line-profile data of Mathias et al. (1994) have been re-analyzed by Aerts (1996). She finds $\ell = 2$, $m = -1$ for f_1 and $\ell = 2$, $m = -2$ for f_3 , but $\ell = 3$, $m = +1$ for f_4 . Thus, according to Aerts (1996), the triplet f_1, f_4, f_3 does not consist of three m states of the same ℓ . For f_2 , Aerts (1996) gets $\ell = 2$ or 3 and $m = 0$. Note that both these possibilities contradict Smith's (1980) finding of $\ell = 0$ for this mode. Another difference between these two investigations is that Smith (1980) determines the star's equatorial velocity of rotation, V_e , to be equal to 75 km s^{-1} , while Aerts (1996) finds $V_e = 30 \text{ km s}^{-1}$.

The only constraint which follows from these discrepant results is that the f_1 mode is nonradial, with ℓ equal to either 1 or 2.

3. The triplet

Any attempt to understand the frequency spectrum of 12 (DD) Lac must begin with the equidistant triplet f_1, f_4, f_3 . We shall consider the following three possibilities of accounting for the

Table 2. The four cases of accounting for the f_1, f_4, f_3 triplet when $\ell = 2$

case:	1	2	3	4
m				
-2	f_3			f_3
-1	f_4	f_3		
0	f_1	f_4	f_3	f_4
1		f_1	f_4	
2			f_1	f_1

triplet: (1) true rotational splitting of an $\ell = 1$ or 2 mode, (2) an roAp-like rotational splitting, and (3) nonlinear phase lock.

In addition to the value of the central frequency, f_4 , the triplet can be characterized by the mean separation,

$$S = (f_3 - f_1)/2, \quad (1)$$

and the asymmetry,

$$\Delta f = f_4 - (f_1 + f_3)/2. \quad (2)$$

Taking the values of the frequencies from Table 1, we get $S = 0.15544 \pm 0.00021$ and $\Delta f = -0.00014 \pm 0.00029 \text{ d}^{-1}$.

3.1. True rotational splitting

As we showed in Sect. 2.4, the spherical harmonic degree of the f_1 mode is either 1 or 2. In the case of rotational splitting, the f_4 and f_3 modes will both have ℓ also equal to 1 or 2. Since for a given ℓ there are $2\ell + 1$ spherical harmonic orders, m , there is only one possibility of accounting for the triplet if $\ell = 1$, and four possibilities if $\ell = 2$. If $\ell = 1$, the order of frequencies in the triplet implies $m = +1$ (retrograde) for f_1 , 0 for f_4 , and -1 for f_3 . Note that this case is the only one consistent with the identification of ℓ from the amplitude ratios.

The four possible cases of accounting for the triplet when $\ell = 2$ are listed in Table 2.

A number of modes of $\ell = 1$ or 2 and $m = -1, 0$ or 1 with frequencies close to f_4 are unstable in models of 12 (DD) Lac in the range of effective temperature and mass allowed by the position of the star in the $\log T_{\text{eff}} - \log g$ plane. An example is presented in Fig. 3. In this figure, computed frequencies of two $\ell = 1$, $m = 0$ modes are plotted together with f_4 (horizontal solid line). The designations p_1 and g_1 refer to the properties of the modes on ZAMS, where the p - and g -mode spectra are separated in frequency.

As can be seen from Fig. 3, f_4 can be fitted with the frequency of the p_1 mode in the whole range of T_{eff} . On the other hand, for the g_1 mode such fit is possible only at the lower limit of the temperature range and for the lowest-mass models which have $\log g$ still consistent with the observed one. In addition, an $\ell = 1$, $m = 0$, p_2 mode in models with $\log T_{\text{eff}} \approx 4.39$ and $M > 13 M_{\odot}$ (not shown in Fig. 3) also has its frequency close to f_4 .

Having identified the modes that could reproduce f_4 (those shown in Fig. 3 and many others), we varied the rotation frequency, Ω , until computed frequencies of the outlying members

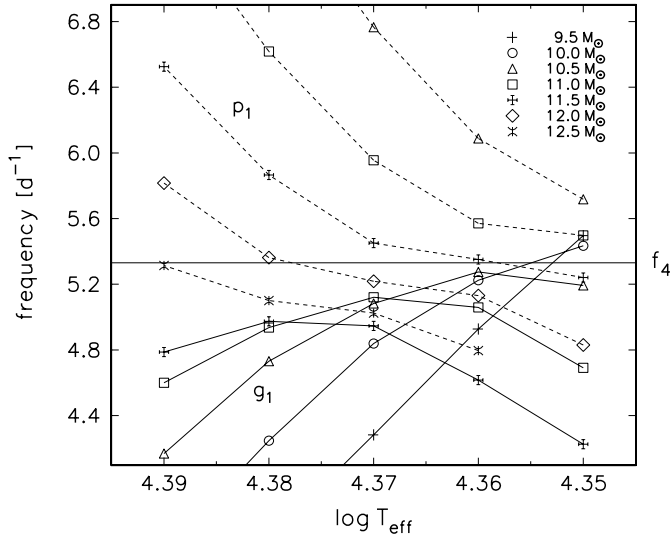


Fig. 3. Computed frequencies of two $\ell = 1$, $m = 0$ modes, compared with f_4 , the central frequency of the triplet (horizontal solid line). The designations p_1 and g_1 refer to the behavior of the modes in the ZAMS models

Table 3. Reproducing observed frequencies: parameters of the models

ℓ	m	n	$\log T_{\text{eff}}$	M	$\log L$	V_e	$\log g$	$\log t$	X_c	Δf	ref
1	0	g_1	4.350	10.22	3.98	94	3.81	7.17	0.27	0.020	
1	0	p_1	4.370	11.84	4.21	114	3.72	7.10	0.21	0.028	A
2	-1	g_1	4.350	10.44	4.03	67	3.77	7.17	0.23	0.003	B
2	0	g_1	4.350	10.31	4.01	61	3.79	7.17	0.24	0.004	
2	-1	p_0	4.370	12.47	4.30	91	3.65	7.09	0.15	0.017	
2	-1	p_0	4.350	11.58	4.21	84	3.64	7.14	0.12	0.018	
2*	0	p_0	4.370	12.24	4.28	40	3.68	7.10	0.16	0.010	C
2	0	p_0	4.370	12.28	4.28	80	3.67	7.09	0.16	0.004	
2	0	p_0	4.350	11.36	4.18	77	3.66	7.15	0.13	0.002	D
2	1	p_0	4.390	13.15	4.39	73	3.71	7.04	0.19	0.010	
2	1	p_0	4.370	12.13	4.26	70	3.69	7.10	0.17	0.010	

of the triplet, f_1 and f_3 , were also fitted. The rule we adopted was that the observed mean separation of the triplet, S , should be reproduced exactly. The interaction between rotation and pulsation was treated as in Soufi et al. (1998), except that only terms up to quadratic in Ω were kept in the perturbation treatment. The effect of near degeneracy of modes differing in ℓ by 2 was taken into account.

Out of a large number of models computed in this way, we selected those which (1) had the smallest asymmetry, Δf , and (2) reproduced – at least approximately – the two frequencies outside the triplet, f_2 and f_6 . The parameters of these models are presented in Table 3. The first three columns identify the f_4 mode (the asterisk indicates case 4 of Table 2), V_e is the equatorial velocity of rotation in km s^{-1} , t is the time in years elapsed since ZA, X_c is the core hydrogen content; the remaining columns should be self-explanatory. The four cases discussed below are indicated in the last column (see also Fig. 2).

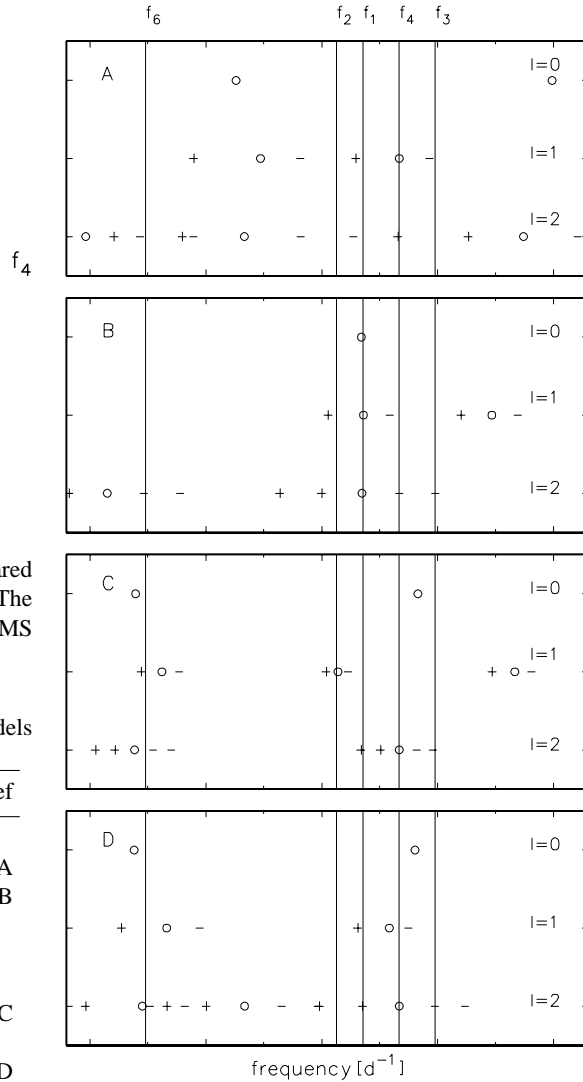


Fig. 4. Reproducing observed frequencies: four models. Parameters of the models are given in Table 3. The $m = 0$ modes are plotted with open circles, the $m > 0$ (retrograde) modes, with plus signs, and the $m < 0$ modes, with minus signs

For the four cases, A, B, C, and D, the computed frequencies of all $\ell \leq 2$ modes that are unstable in the frequency range from 3.9 to 6.1 d^{-1} are compared with the observed ones in Fig. 4. Frequencies of the prograde modes ($m < 0$) are plotted with minus signs, those of the retrograde ones, with plus signs.

As can be seen from Fig. 4, the number of unstable modes is much greater than the number of the observed ones. This problem is common to all linear pulsation analyses (see, for example, Dziembowski 1997).

In Table 3, the computed asymmetry of the triplet is always greater than the observed one. When f_4 is identified with an $\ell = 1$ mode, computed Δf is about two orders of magnitude greater than observed. Case A, in which f_4 is identified with the $\ell = 1$, $m = 0$, p_1 mode, is an example. In case B, with f_4 identified as the $\ell = 2$, $m = -1$, g_1 mode, $\Delta f = 0.003 \text{ d}^{-1}$. Although quite small, this value is still an order of magnitude

Table 4. The frequencies and the magnetic and rotational frequency shifts, in d^{-1} , for low-order $\ell = 1$ modes

n	f	δ_{mag}	δ_{rot}^1	δ_{rot}^2
g_1	4.50	3.39E-06	3.53E-02	3.33E-02
p_1	5.21	8.80E-06	1.14E-01	1.77E-02
p_2	6.13	2.64E-04	1.33E-02	5.86E-02

too large. Case C represents the best fit to all five frequencies. Now, however, $\Delta f = 0.010 \text{ d}^{-1}$. Finally, there is case D, with the smallest Δf in Table 3. In its vicinity we found a model with $\Delta f < 0$. But in this model, the two remaining frequencies, f_2 and f_6 , were not well fitted. It is possible, however, that the situation could be improved by changing the heavy elements content.

3.2. Oblique magnetic pulsator

Equally split triplets are observed in rapidly oscillating Ap (roAp) stars such as HD 24712 = DO Eri (Kurtz et al. 1989). According to the oblique pulsator model, first proposed by Kurtz (1982), an equally split triplet is seen in the observer's frame if a single $\ell = 1$ mode has its axis of symmetry (the pulsation axis) inclined to the rotation axis. In such a case Δf is exactly equal to zero and $S = f_{\text{rot}}$, where f_{rot} is the rotation frequency of the pulsation axis. An equally spaced quintuplet, separated by f_{rot} , would be seen if an $\ell = 2$ mode were excited instead of the $\ell = 1$ mode. In general, the number of frequencies seen by the observer will be $2\ell + 1$ for each mode of degree ℓ .

In the context of the β Cephei stars, the oblique pulsator model has been recently invoked by Shibahashi & Aerts (1998) in their attempt to account for the frequency spectrum of β Cep itself. In order to find out whether this model could be also applied to the present case, we compared the effect of a magnetic field and that of rotation on the frequencies of low-order, low-degree modes. Sample results, computed for three $\ell = 1$ modes in a $12 M_{\odot}$ model with $\log T_{\text{eff}} = 4.37$ and $\log L = 4.2385$, are presented in Table 4. Following Dziembowski & Goode's (1996) investigation of magnetic effects in roAp stars, we assumed a dipole magnetic field. In column 3 are given the magnetic frequency shifts, δ_{mag} , due to a $B_p = 1 \text{ kG}$ field for $m = 0$ in the magnetic reference system. The magnetic shifts scale roughly as B_p^2 . The rotational shifts, listed in columns 4 and 5, were computed for $V_e = 91 \text{ km s}^{-1}$; the linear shifts, δ_{rot}^1 , are for $m = 1$, the quadratic ones, δ_{rot}^2 , are for $m = 0$. The linear shifts scale as $\sim mV_e$, while the quadratic ones, as $\sim Q_l^m V_e^2$, where $Q_l^m = [\ell(\ell + 1) - 3m^2]/[4\ell(\ell + 1) - 3]$. Therefore, even for the lowest V_e in Table 3, δ_{mag} remains an order of magnitude smaller than either δ_{rot}^1 or δ_{rot}^2 .

This situation is typical for low-order modes. In roAp stars at similar field intensities the magnetic corrections are much larger. The reason is that the modes excited in these stars are acoustic modes of very high radial orders ($n > 20$). Such modes propagate into the outermost layers in which the magnetic per-

turbation is large because the perturbing effect scales as B^2/P , where P is the gas pressure, and P grows much more rapidly inward than B^2 . In these magnetically perturbed layers the low degree modes are evanescent. In the model considered here the magnetic perturbation becomes comparable with the rotational one for $n \geq 7$.

Application of the oblique pulsator model to 12 (DD) Lac in order to account for the f_1, f_4, f_3 triplet would thus require postulating unrealistically strong magnetic field, much stronger than that observed in the helium star δ Ori C, which has the strongest known magnetic field in this part of the H-R diagram (Bohlender et al. 1987). In the case of weak magnetic perturbation, the departure from a single Y_ℓ^m dependence in the rotational reference system for the individual eigenmodes is small. Thus, given the lack of observations of magnetic field in 12 (DD) Lac, we may contemplate only a weak amplitude modulation or, equivalently, only small amplitudes of the side peaks in the triplet. This is not what we see. In addition, there is the following difficulty with the model: since the f_2 and f_6 terms are both singlets, they must both be radial. For this, however, the observed frequency separation between them is too small, as can be seen from Fig. 4.

For all these reasons we regard the oblique magnetic pulsator explanation of the triplet as the least likely. However, we cannot reject it altogether because we made a specific assumption about the field geometry.

3.3. Nonlinear phase locking

Buchler et al. (1995) have investigated the nonlinear behavior of rotationally split $\ell = 1$ mode. They found that – depending on the parameters of the model and the specific triplet considered – the predicted amplitudes are constant in time or exhibit long-term modulations. When all three component modes are excited and the amplitudes are constant then nonlinear phase locking causes the frequencies to appear exactly equidistant. For 12 (DD) Lac, this mechanism was recently considered by Goupil et al. (1998). The conclusion of their work is that in this case the phase lock is marginally possible.

The phase lock leading to exactly equidistant frequency separations may occur for any three modes whose linear frequencies obey the approximate relation $\nu_2 \approx (\nu_1 + \nu_3)/2$, provided that the integral of $(Y_1 Y_3)^* Y_2^2$, where Y_k 's denote spherical harmonics of the respective modes, is not equal to zero. This implies that the azimuthal orders of the three modes must satisfy the condition $2m_2 = m_1 + m_3$. Note that this condition is not fulfilled in the case of Aerts' (1996) ℓ and m identifications for the f_1, f_4, f_3 triplet (see above, Sect. 2.4). Consequently, her suggestion that “mode 4 might be excited through resonant coupling between modes 1 and 3” is invalid.

The nonlinear phase locking shifts the frequencies from their positions predicted by the linear theory. These shifts would have to be determined by means of nonlinear calculations and taken into account in fits such as those shown in Figs. 3 and 4. An order of magnitude example of this can be found in Goupil et al. (1998).

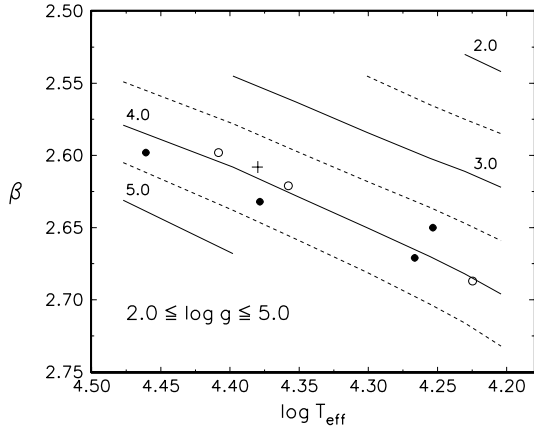


Fig. A1. Lines of constant $\log g$ in the $\log T_{\text{eff}} - \beta$ plane from Smalley & Dworetsky’s (1995) grid of synthetic β indices. Dashed lines represent half-integer values of $\log g$. Also shown are early-B components of seven binary systems (filled and open circles) and 12 (DD) Lac (plus sign), plotted using the photometric $\log T_{\text{eff}}$ values and the observed β . The binary systems are identified in the text

4. Summary

Of the three possibilities of accounting for the equidistant triplet, the oblique magnetic pulsator model is the least likely one because it would require excessively strong dipolar field or a special field geometry. The true rotational splitting may be the answer but only if ℓ were equal to 2. This is because for $\ell = 1$, the computed Δf is always about two orders of magnitude greater than observed. The true rotational splitting is thus in conflict with the ℓ values derived in Sect. 2.4 from the amplitude ratios. For $\ell = 2$, computed Δf is close to the observed one for very specific model parameters, namely, in the vicinity of point D in Fig. 2. Since point D deviates from the observed position of 12 (DD) Lac by one σ in $\log T_{\text{eff}}$ and about 0.5σ in $\log g$, improving the accuracy of $\log T_{\text{eff}}$ and $\log g$ may lead to eliminating the true rotational splitting altogether. The only remaining solution would then involve nonlinear phase lock. This would be bad news for asteroseismology because the nonlinear calculations are much more complicated than the linear ones.

Acknowledgements. This work was supported by KBN grants 2 P03D 016 11 and 2 P03D 014 14.

Appendix A: Calibration of $\log g$

Fig. A1 shows $\log g$ on the $\log T_{\text{eff}} - \beta$ plane for the effective temperature range of early B stars. The solid and dashed lines (integer and half-integer values of $\log g$, respectively) are from Smalley & Dworetsky’s (1995) grid. The filled and open circles represent early-B components of binary systems for which empirical $\log g$ values are known, and the plus sign is 12 (DD) Lac. These points were plotted using observed β indices and the photometric effective temperatures, derived from c_0 and β via the calibration of Napiwotzki et al. (1993), mentioned in Sect. 2.1. In order of decreasing $\log T_{\text{eff}}$, objects with known $\log g$ are CW Cep AB (Crawford & Barnes 1970, Giménez et al. 1990,

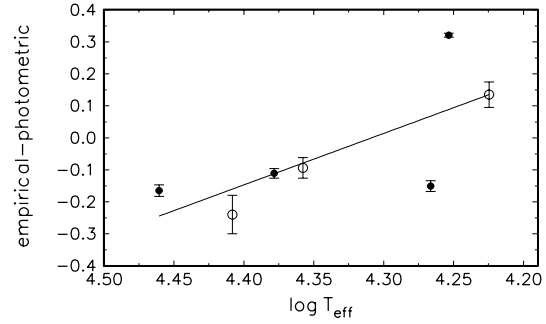


Fig. A2. The difference between the empirical and photometric $\log g$ values for the binary systems shown in Fig. A1, plotted as a function of the photometric $\log T_{\text{eff}}$. The error bars represent standard deviations of the empirical values. The solid straight line was fitted to the points by the method of least squares

Clausen & Giménez 1991), α Vir A (Sterken & Jerzykiewicz 1993), QX Car AB (Andersen et al. 1983, Giménez et al. 1986), 16 Lac (Sterken & Jerzykiewicz 1993), V539 Ara A (Crawford et al. 1971, Grønbech & Olsen 1976, 1977), CV Vel AB (Clausen & Grønbech 1977, Balona 1994) and HR 2680 (Grønbech & Olsen 1976, 1977). The references in parentheses contain the *wavy* and β photometry we used. For the binaries with nearly equal components, denoted AB, we used combined light photometry. For α Vir A, V539 Ara A and HR 2680, we corrected the observed indices for the light of the fainter component; in the case of HR 2680, these duplicity corrections were very small. No corrections were required for 16 Lac. Note that in this figure 12 (DD) Lac is plotted with its photometric $\log T_{\text{eff}} = 4.380$.

For the binary systems, the $\log g$ values read off Fig. A1, which we shall refer to as “photometric,” can be compared with the empirical ones. For components of the SB2 eclipsing binaries CW Cep, QX Car, V539 Ara and CV Vel (filled circles), the empirical $\log g$ values have been listed by Andersen (1991). For the primary component of Spica (the leftmost open circle), $\log g$ can be derived from the mass and radius obtained by combining the spectrographic and interferometric orbits and the angular diameter (Herbison-Evans et al. 1971). Finally, for the primary components of the SB1 eclipsing binaries 16 Lac and HR 2680 (the other two open circles), the empirical values have been determined by Jerzykiewicz (1994). In the latter two cases, a mass had to be assumed to obtain $\log g$, but the results were insensitive to the assumed mass. Taking straight means for the nearly equal-components binaries CW Cep, QX Car and CV Vel, we present the comparison in Fig. A2, where the difference between the empirical and photometric $\log g$ values is plotted as a function of the photometric effective temperature. The error bars were plotted using standard deviations of the empirical values. For 16 Lac and HR 2680, the standard deviations are equivalent to changing the assumed mass by $2 M_{\odot}$. The solid straight line was derived by the method of least squares. Equal weights were given to the points in the least-squares solution because the scatter in Fig. A2 is clearly not correlated with the standard deviations of the empirical $\log g$ values.

The photometric $\log g$ value of 12 (DD) Lac read off Fig. A1 is equal to 3.87. Taking into account the difference “empirical *minus* photometric,” implied for $\log T_{\text{eff}} = 4.380$ by the straight line in Fig. A2, we correct this to $\log g = 3.76 \pm 0.15$, where the standard deviation is that of the least-squares fit to the $\log g$ differences. Adopting this standard deviation we assume that the scatter in Fig. A2 is caused mainly by errors of the photometric indices.

References

- Abrami A., Bakos G., Broglia P., et al., 1957, *Nat* 180, 1112
 Adams W.S. 1912, *ApJ* 35, 179
 Aerts C. 1996, *A&A* 314, 115
 Andersen J. 1991, *A&AR* 3, 91
 Andersen J., Clausen J.V., Nordström B., Reipurth B., 1983, *A&A* 121, 271
 Balona L.A., 1994, *MNRAS* 268, 119
 Bohlender D.A., Brown D.N., Landstreet J.D., Thompson I.B., 1987, *ApJ* 323, 325
 Buchler J.R., Goupil M.J., Serre T., 1995, *A&A* 296, 405
 Clausen J.V., Giménez A., 1991, *A&A* 241, 98
 Clausen J.V., Grønbech B., 1977, *A&A* 58, 131
 Code A.D., Davis J., Bless R.C., Hanbury Brown R., 1976, *ApJ* 203, 417
 Crawford D.L., Barnes J.V., 1970, *AJ* 75, 952
 Crawford D.L., Barnes J.V., Golson J.C., 1971, *AJ* 76, 621
 Cugier H., Dziembowski W.A., Pamyatnykh A.A., 1994, *A&A* 291, 143
 Dziembowski W.A., 1997, In: Provost J., Schmider F.X. (eds.) *Sounding Solar and Stellar Interiors*. IAU Symposium No. 181, p. 317
 Dziembowski W.A., Goode P.R., 1996, *ApJ* 458, 338
 Dziembowski W.A., Jerzykiewicz M., 1996, *A&A* 306, 436 (Paper I)
 Dziembowski W., Pamyatnykh A.A., 1993, *MNRAS* 262, 204
 Giménez A., Clausen J.V., Jensen K.S., 1986, *A&A* 159, 157
 Giménez A., García J.M., Rolland A., Clausen J.V., 1990, *A&AS* 86, 259
 Goupil M.J., Dziembowski W.A., Fontaine G., 1998, *Balt. Astron.* 7, 21
 Grønbech B., Olsen E.H., 1976, *A&AS* 25, 213
 Grønbech B., Olsen E.H., 1977, *A&AS* 27, 443
 Guthnick P., 1919, *Astron. Nachr.* 208, 219
 Herbison-Evans D., Hanbury Brown R., Davis J., Allen L.R., 1971, *MNRAS* 151, 161
 Iglesias C.A., Rogers F.J., 1996, *ApJ* 464, 943
 Jager C. de, 1963, *BAN* 17, 1
 Jerzykiewicz M., 1978, *Acta Astron.* 28, 465
 Jerzykiewicz M. 1994, In: van Woerden H. (ed.) *XXII GA of the IAU Astronomy Posters*. Twin Press, Sliedrecht, p. 238
 Kurtz D.W., 1982, *MNRAS* 200, 807
 Kurtz D.W., Matthews J.M., Martinez P., et al., 1989, *MNRAS* 240, 881
 Kurucz R.L., 1979, *ApJS* 40, 1
 Lesh J.R., 1968, *ApJS* 17, 371
 Mathias P., Aerts C., Gillet D., Waelkens C., 1994, *A&A* 289, 875
 Napiwotzki R., Schönberner D., Wenske V., 1993, *A&A* 268, 653
 Pigulski A., 1994, *A&A* 292, 183
 Sato N., 1973, *Ap&SS* 24, 215
 Sato N., 1977, *Ap&SS* 48, 453
 Sato N., 1979, *Ap&SS* 66, 309
 Schmidt E.G., 1979, *AJ* 84, 1739
 Schmidt E.G., Taylor D.J., 1979, *AJ* 84, 1193
 Shibahashi H., Aerts C., 1998, In: *New Eyes to See Inside the Sun and Stars*. IAU Symp. No. 185, in press
 Smalley B., Dworetzky M.M., 1995, *A&A* 293, 446
 Smith M.A., 1980, *ApJ* 240, 149
 Soufi F., Goupil M.J., Dziembowski W.A., 1998, *A&A* 334, 911
 Stebbins J., 1917, *Pop. Astr.* 25, 657
 Sterken C., Jerzykiewicz M., 1993, *Space Sci. Rev.* 62, 171
 Struve O., 1951, *ApJ* 113, 589
 Young R.K., 1915, *Publ. Dom. Obs. Ottawa* 3, 65